# Effects of Cu coverage on the magnetic anisotropy of Co/Cu(001)

**Article** *in* Physical Review B · October 1999

DOI: 10.1103/PhysRevB.60.9539



**2 authors:**

Vladimir Gavrilenko
VLEXCO LLC
**106** PUBLICATIONS **1,248** CITATIONS
SEE PROFILE

Ruqian Wu
University of California, Irvine
**246** PUBLICATIONS **6,249** CITATIONS
SEE PROFILE

# Effects of Cu coverage on the magnetic anisotropy of Co/Cu(001)

V. I. Gavrilenko and Ruqian Wu
*Department of Physics and Astronomy, California State University, Northridge, California 91330-8268*
(Received 1 December 1998; revised manuscript received 26 April 1999)

Using the full-potential linearized augmented plane wave method, the magnetocrystalline anisotropy (MCA) energies of the Co/Cu(001), Cu/Co/Cu(001), and 2Cu/Co/Cu(001) systems are investigated. With the generalized gradient approximation for the exchange-correlation energy/potential, the optimized atomic structures are remarkably improved from those obtained with the local-density approximation. The negative uniaxial MCA energy of Co/Cu(001) ($-0.61$ meV per Co adatom) changes to positive for Cu/Co/Cu(001) (0.54 meV per Co adatom) and for 2Cu/Co/Cu(001) (0.21 meV per Co adatom). This indicates that the Cu overlayers turn the magnetization of Co from the in-plane direction to the perpendicular axis, a conclusion which agrees with experiments. By contrast, the in-plane coefficient of MCA energy appears to be quite stable in these systems. [S0163-1829(99)03737-6]

## I. INTRODUCTION

The determination of magnetocrystalline anisotropy (MCA) energies in various transition metal ultrathin films has attracted extensive attention in the last decade.[1–6] Recent experiments found that magnetic anisotropy energy strongly depends on change in environment. For example, the in-plane easy axis of Co films on Cu(001), Cu(110), and Cu(111) can be turned to the perpendicular direction when they are capped by a few monolayers of nonmagnetic atoms such as Cu, Pd, Ag, or Au.[2,3] Weber *et al.* reported that magnetic anisotropy of Cu/Co thin films is strongly affected by the nonmagnetic vacuum/Cu interface even when it is displaced by as much as 16 atomic monolayer from the Co layers.[5] Hope *et al.* found that a submonolayer Cu coverage can completely reverse the in-plane 90° easy axis when depositing Cu overlayers onto the Co gas-dosed Co/Cu(110) surface.[6] By growing fcc Co films on a curved Cu(001) substrate, Kawakami *et al.* found that the magnetic anisotropy strength depend almost linearly on the step density.[7]

It is known that the magnetocrystalline anisotropy energy results mainly from spin-orbit coupling (SOC) interactions among the occupied and unoccupied states. Highly stable results of uniaxial MCA energies can be obtained now from the first-principles electronic structure calculations by treating the SOC Hamiltonian either self-consistently or perturbatively.[8] By using the state-tracking[9] and torque approaches[10] based on the local-density full-potential linearized augmented plane wave (FLAPW) method, Zhong *et al.* and Kim *et al.* successfully reproduced and explained the effects of Cu coverage on the magnetic anisotropy behaviors of Co/Cu(110) and Co/Cu(111).[11,12] Szunyogh *et al.*, with the local-density screened Korringa-Kohn-Rostoker in atomic sphere approximation (SKKR-ASA) and the force theorem, studied the magnetic anisotropy energies of several Co/Cu(001) systems capped by an additional monolayer of Cu, Ag, Rh, Au, or Pt.[13] A large magnetostrictive coefficient is found ($\lambda_{001}$ is $-57\times10^{-6}$) at the Co/Cu(001) interface in previous calculations,[14,15] which indicates that the MCA energy strongly depends on the interfacial structural relaxation.

Due to the known deficiency of the local-density approximation (LDA), the Co/Cu interlayer distances in all previous calculations were underestimated by several percents.[11,14,15] This certainly makes the calculated MCA energies questionable with geometries optimized through LDA calculations. In addition, since the MCA energy is very sensitive to small changes in the band structure near the Fermi level, it is important to investigate effects of the charge- and spin-density corrugations.

In this paper, we report results of structural, electronic, and magnetic properties of Co/Cu(001), Cu/Co/Cu(001), and 2Cu/Co/Cu(001), using the generalized gradient approximation (GGA).[16] The Co/Cu and Cu/Cu interlayer distances are found to be significantly larger than the corresponding LDA results. The calculated uniaxial MCA energies are $-0.61$ meV, $+0.54$ meV, and $+0.21$ meV for Co/Cu(001), Cu/Co/Cu(001), and 2Cu/Co/Cu(001), respectively. Reliable results are also obtained for the in-plane MCA coefficients.

## II. METHOD

The FLAPW method[17] solves the single-particle Kohn-Sham equations self-consistently, with a fully relativistic treatment for both core and valence states. To simplify the calculations, the SOC Hamiltonian ($H_{SOC}=\xi\mathbf{s}\cdot\mathbf{L}$) for the valence states is invoked second-variationally, with $z$-spin magnetization. Since the strength of $H_{SOC}$ is much weaker than that of the crystal-field interaction in $3d$-transition-metal systems, we neglected the spin-flipping effect and projected the wave functions, charge densities, and potentials to two separate spin channels as done in semirelativistic calculations.[8]

No shape approximation is assumed for charge, potential, and wave functions. The GGA formula of Ref. 16 is adopted to describe the exchange-correlation effects. In the muffin-tin region, spherical harmonics with a maximum angular momentum of eight are used to expand the charge, potential, and wave functions. In the interstitial area, plane waves with energy cutoffs of 150 Ry (for the charge and potential) and 14 Ry (for the variational bases) are employed. Self-consistency is assumed when the root-mean-square distances between the input and output charge and spin densities be-

 

come less than $1.0\times10^{-4}$ electrons/a.u.$^3$ 300 **k** points in the 1/8 irreducible part of the two-dimensional Brillouin zone are used for integrals in the reciprocal space.

The Cu(001) substrate is modeled by a five-layer Cu(001) slab. We studied (1) the clean Co/Cu(001) surface, (2) the Cu/Co/Cu(001), and (3) the 2Cu/Co/Cu(001) systems to investigate the effects of the Cu cap layers. Co and Cu adatoms are placed pseudomorphically on both sides of the slab to retain the inversion symmetry. The equilibrium atomic structures are determined through total energy and atomic force calculations, with a criterion that requires the force on each atom to be smaller than $2\times10^{-3}$ Hartree/a.u.

For a system with fourfold symmetry with respect to its surface normal, the magnetocrystalline anisotropy energy, $E_{MCA}$, can be expressed in the lowest nonvanishing order of the polar and azimuth angles ($\theta$ and $\phi$, respectively) as[2,18]

$$E_{MCA}=K_1\sin^2\theta+K_2\sin^2(2\phi)\sin^4\theta. \tag{1}$$

Here $K_1$ and $K_2$ are the coefficients of the leading uniaxial and in-plane contributions to $E_{MCA}$, respectively. They can be determined through angular derivatives of $E_{MCA}$ ($T=dE_{MCA}/d\theta$, where $T$ is the torque) as

$$K_1=T(\theta=45°,\phi=0°),\quad K_2=T(\theta=45°,\phi=45°)-K_1. \tag{2}$$

Here, $T$ is calculated through the expectation value of the angular derivative of $H_{SOC}$ as

$$T(\theta,\phi)=\sum_{i\in\text{occ}}\left\langle i\left|\frac{\partial H_{SOC}(\theta,\phi)}{\partial\theta}\right|i\right\rangle \tag{3}$$

and

$$H_{SOC}=\begin{pmatrix}H_{SOC}^{\uparrow\uparrow} & H_{SOC}^{\uparrow\downarrow}\\ H_{SOC}^{\downarrow\uparrow} & H_{SOC}^{\downarrow\downarrow}\end{pmatrix}. \tag{4}$$

Here $H_{SOC}^{\uparrow\uparrow}=\cos\theta L_z+\sin\theta(A+B)/2$; $H_{SOC}^{\downarrow\downarrow}=-\cos\theta L_z-\sin\theta(A+B)/2$; $H_{SOC}^{\uparrow\downarrow}=\cos^2(\theta/2)A-\sin^2(\theta/2)B-\sin\theta L_z$; and $H_{SOC}^{\downarrow\uparrow}=\cos^2(\theta/2)B-\sin^2(\theta/2)A-\sin\theta L_z$ (with $A=e^{i\phi}L_-$ and $B=e^{-i\phi}L_+$). The spin-flipping terms (i.e., $H_{SOC}^{\downarrow\uparrow}$ and $H_{SOC}^{\uparrow\downarrow}$), do not affect charge density much but may contribute significantly to the MCA energy.[8]

$K_1$ can be determined quite satisfactorily for most magnetic thin films through the first-principles calculations using torque, force theorem, or total-energy approaches.[8] By contrast, $K_2$ is very small (a few $\mu$eV/atom) and thus is very difficult for force theorem and total-energy approaches.

## III. ATOMIC STRUCTURE AND MAGNETISM

To demonstrate the advantages of the GGA approach for structural optimizations, we first calculated the fcc bulk Cu using both GGA and LDA density-functional formulas. The calculated ratios of theoretical and experimental lattice constants ($r=a_{theo}/a_{exp}$, with $a_{exp}=6.83$ a.u.) are 1.004 with GGA and 0.975 with LDA, respectively. Clearly, the GGA result (0.4% larger) is much better than the LDA counterpart (2.5% smaller) compared to the experimental data. Our test calculations indicated that GGA systematically improves the reliability of the calculated lattice constants, cohesion energies, and bulk moduli for all $3d$ transition metals.[19] For example, the calculated bulk modulus ($B$) for the bulk fcc Cu with GGA, $B_{GGA}$, is 132.7 GPa, a value that agrees excellently with experiment for fcc bulk Cu, 134.3 GPa.[20] By contrast, the bulk modulus calculated using LDA for the fcc bulk Cu is 161.7 GPa, which is obviously much too large.

TABLE I. The calculated equilibrium vertical positions ($z$, in a.u.) spin ($M$), and orbital ($L_z$) magnetic moments (in $\mu_B$) of the Cu/Co/Cu(001) systems.

| | Cu(1) | Cu(2) | Cu(3) | Co | Cu(4) | Cu(5) |
|---|---|---|---|---|---|---|
| $Co/Cu_5$ | | | | | | |
| $z$ | 0.0 | 3.47 | 6.98 | 10.43 | | |
| $M$ | −0.001 | −0.01 | 0.017 | 1.92 | | |
| $L_z$ | 0.00 | −0.004 | 0.002 | 0.118 | | |
| $Cu/Co/Cu_5$ | | | | | | |
| $z$ | 0.0 | 3.48 | 7.00 | 10.50 | 13.93 | |
| $M$ | 0.002 | −0.007 | 0.02 | 1.74 | 0.025 | |
| $L_z$ | 0.00 | −0.005 | 0.001 | 0.117 | 0.002 | |
| $Cu_2/Co/Cu_5$ | | | | | | |
| $z$ | 0.0 | 3.48 | 7.00 | 10.49 | 13.95 | 17.45 |
| $M$ | 0.001 | −0.008 | 0.02 | 1.74 | 0.037 | −0.004 |
| $L_z$ | 0.00 | −0.002 | 0.001 | 0.099 | 0.002 | 0.00 |

For all the thin films, we used an in-plane lattice constant, 4.83 a.u. (corresponding to $a=6.83$ a.u. in the cubic fcc cell). The vertical positions of all the atoms in the unit cell were adjusted according to their atomic forces. The calculated equilibrium $z$ coordinates are presented in Table I. As expected, the Cu/Cu interlayer distance in the interior region remains constant, 3.47–3.48 a.u., in all the systems studied. This value is slightly larger than the measured value, 3.42 a.u., since the GGA-optimized lattice constant for bulk Cu (6.86 a.u.) is 0.4% larger than that used in the lateral plane. By contrast, the average Cu-Cu interlayer distance from LDA calculations is 3.25–3.32 a.u. for Co/Cu(001).[14] Clearly, GGA is more suitable than LDA to optimize that atomic structure of magnetic thin films.

The Cu-Cu interlayer distance at the interfacial region appears to be 1% larger than that in the interior region (3.51 a.u. versus 3.47 a.u.). This indicates that Co induces a slight lattice expansion in the adjacent Cu layers. Here, the surface Co-Cu interlayer distances in Co/Cu(001) and Cu/Co/Cu(001) are 3.43–3.45 a.u. This value is about 10% larger than that obtained in previous LDA calculations, 3.08–3.11 a.u.[14,15] Interestingly, the surface Cu-Cu interlayer distance 3.50 a.u. expands by 1% from that in the interior region. This result agrees excellently with a low-energy electron-diffraction (LEED) experiment that found a slight expansion (1.5%) at the Cu(001) clean surface.[21]

In Figs. 1–3, the calculated valence charge and spin densities of Co/Cu(001), Cu/Co/Cu(001), and 2Cu/Co/Cu(001) are presented, respectively. Strong Co/Cu interfacial interaction can be seen from the charge-density contours around the Co atoms. The profile of contours in the region below the Co plane in Co/Cu(001) is already very similar to that around the interior Cu atoms. Directional bonds are shown between Cu(4)-Co atoms in both Cu/Co/Cu(001) and 2Cu/Co/Cu(001) systems. From the spin-density contours, the Cu-Co

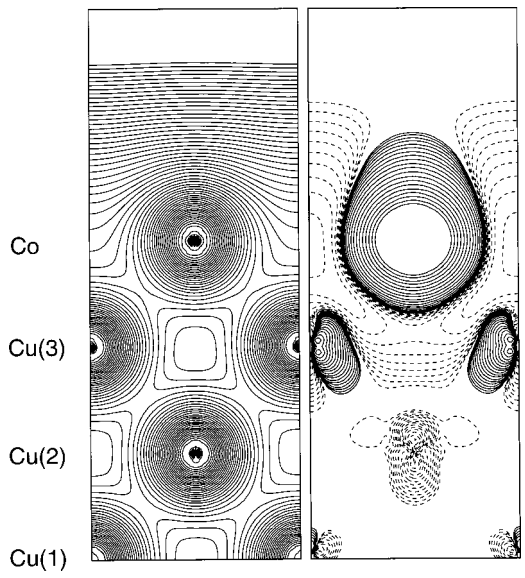


FIG. 1. The calculated valence charge (a) and spin (b) densities of Co/Cu(001). Contours start from $\pm 1\times 10^{-3}e$/a.u.$^3$, and increase successively by a factor of $\sqrt{2}$. Solid and dashed contours in panel (b) denote positive and negative spin densities, respectively.

hybridization can be found to be detrimental to the spin polarization of the Co atom. The area of positive spin density (solid contours) on top of the Co atom in Co/Cu(001) is significantly depressed by the Cu coverage, especially in Cu/Co/Cu(001). The induced spin density in the Cu layers change quickly from the *d*-like to *sp*-like away from the interfacial region. Quantitatively, the calculated spin (orbital) magnetic moments of the Co atom are 1.92 $(0.118)\mu_B$, 1.74 $(0.117)\mu_B$, and 1.74 $(0.099)\mu_B$ in Co/Cu(001), Cu/Co/Cu(001), and 2Cu/Co/Cu(001), respectively. The orbital magnetic moments calculated here, with contributions from the SOC only, are somewhat smaller than the measured value $(0.18\mu_B)$ using the x-ray magnetic circular dichroism sum rules.[22]

Curves of the calculated density of states (DOS) shown in Figs. 4–6 indicate more clearly the interfacial hybridization

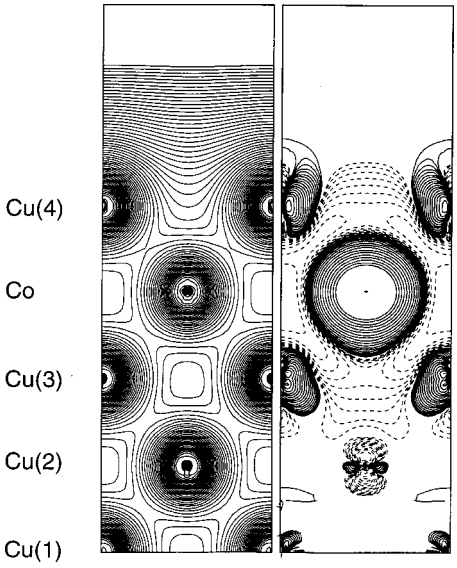


FIG. 2. As in Fig. 1, but for Cu/Co/Cu(001).

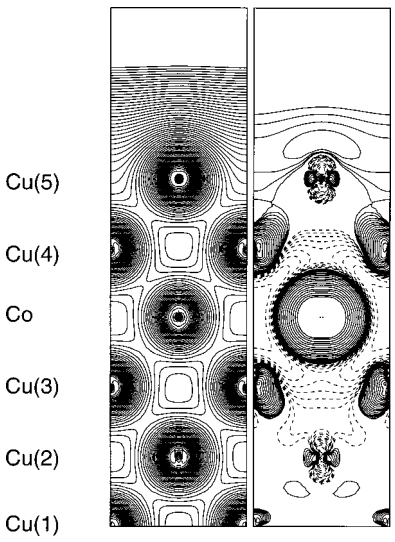


FIG. 3. As in Fig. 1, but for 2Cu/Co/Cu(001).

between the Cu and Co atoms. For the majority-spin part, the Co *d* band overlaps with that of Cu in energy and thus Co-Cu interaction is very similar to Cu-Cu interaction. For the minority-spin part, Cu and Co *d* states hybridize mainly in the occupied region. The Co *d* band in Cu/Co/Cu(001) is significantly broadened from that in Co/Cu(001). Even the DOS of Cu(3) is noticeably affected. From Cu/Co/Cu(001) to 2Cu/Co/Cu(001), the Co-Cu(4) hybridization appears to be weakened by the additional Cu(5) overlayer, which broadens and shifts the Cu(4) *d* band to the low-energy region.

## IV. MAGNETOCRYSTALLINE ANISOTROPY

In Fig. 7, the calculated values of both $K_1$ and $K_2$ coefficients for Co/Cu(001), Cu/Co/Cu(001), and 2Cu/Co/Cu(001) are given versus their numbers of valence electrons (obtained by varying the position of the highest-occupied energy level

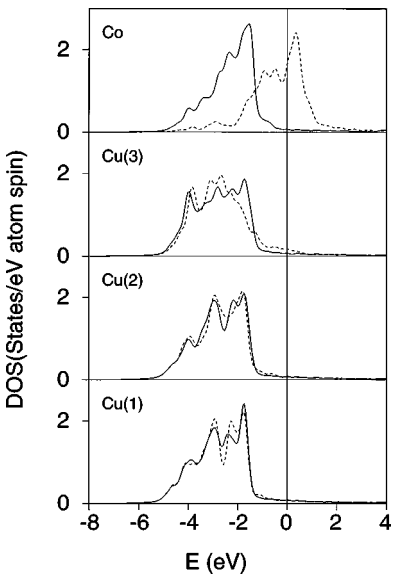


FIG. 4. The calculated density of states for each atom of Co/Cu(001). Solid and dashed lines represent majority and minority spin parts, respectively. Zero on the energy scale represents the Fermi energy.

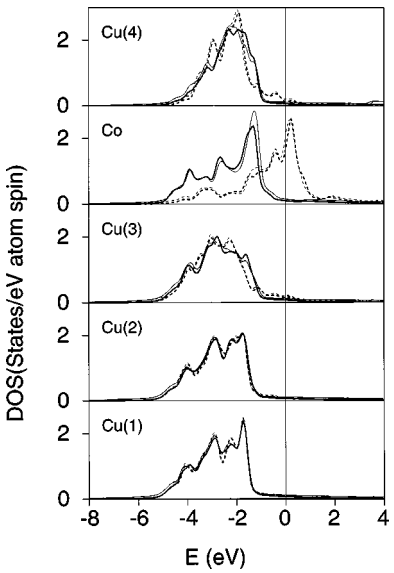


FIG. 5. As in Fig. 4, but for Cu/Co/Cu(001). Thin lines indicate the LDA results.

for each system). For all the systems, both $K_1$ and $K_2$ curves are quite smooth—indicating the numerical stability of the present results of MCA energy determined through the FLAPW method. Test calculations indicated that $K_1$ ($K_2$) is converged to better than 0.05 meV (3 $\mu$eV) with 300 $k$ points in the 1/8 irreducible two-dimensional Brillouin zone.

As was discussed by Zhong *et al.* for Co/Cu(111),[11] the calculated results of $K_1$ change drastically, from $-0.61$ meV per Co atom for Co/Cu(001) to $+0.54$ meV per Co atom in Cu/Co/Cu(001) and, finally, to 0.21 meV per Co atom in 2Cu/Co/Cu(001). These results explain previous experimental observation by Krams *et al.*[2] for Cu/Co/Cu(001) and Engel *et al.*[3] for Co films in other structures, that the nonmagnetic Cu coverage alters the Co magnetization from the lateral plane to the perpendicular axis.

The mechanism of this ''anomalous perpendicular anisotropy'' was discussed by several authors for different

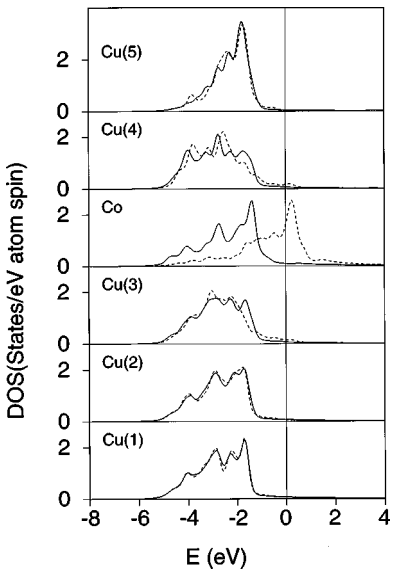


FIG. 6. As in Fig. 4, but for 2Cu/Co/Cu(001).

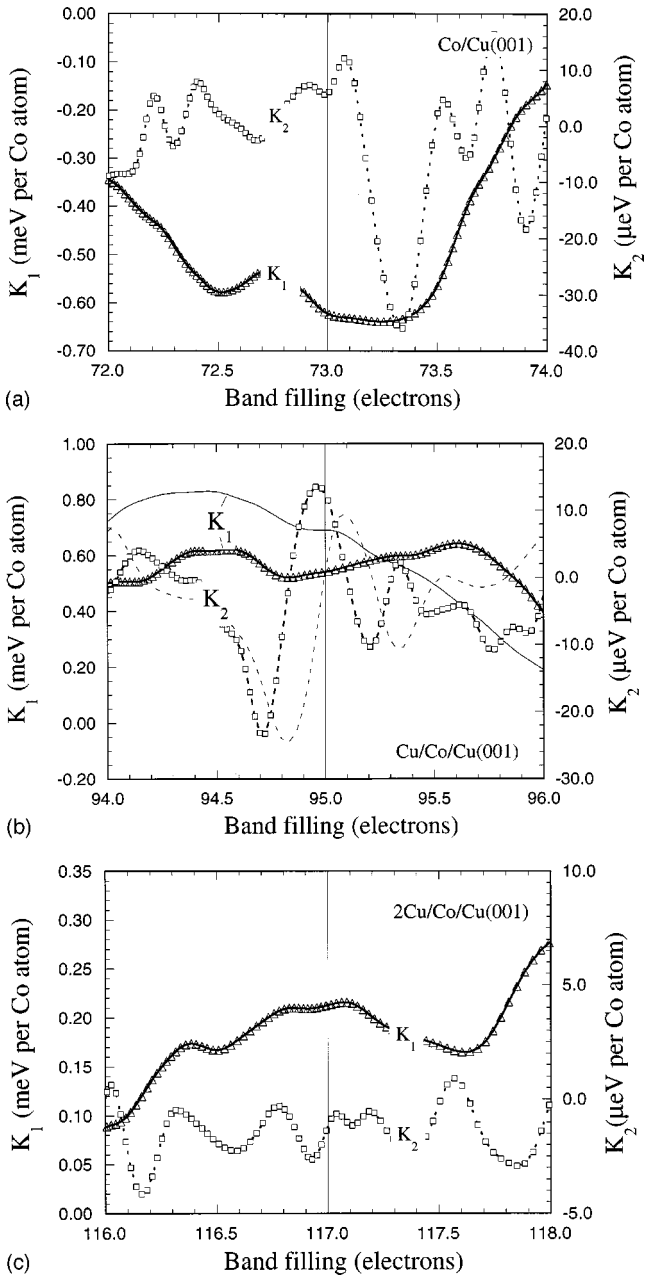


FIG. 7. The calculated MCA energy coefficients for (a) Co/Cu(001), (b) Cu/Co/Cu(001), and (c) 2Cu/Co/Cu(001) versus band filling. Thin lines in panel (b) stand for LDA results using the equilibrium atomic structure optimized through GGA calculations.

systems.[11,13] For Cu/Co/Cu(001), we can start from why Co(001) film has a negative $E_{MCA}$ (i.e., in-plane magnetic anisotropy). From band structure analyses for a free Co(001) monolayer, we pointed out that this was mainly due to the SOC interaction between the occupied $d_{xz,yz}$ states ($m=\pm 1$, where $m$ represents the magnetic quantum number) and the unoccupied $d_{z^2}$ ($m=0$) and $d_{xy}$ ($m=\pm 2$) states at the $\bar{M}$ point in the minority-spin channel. This interaction is drastically weakened when the Co thin film is deposited on the Cu(001) substrate or sandwiched by Cu cap layers. As discussed above, the Cu $d$ states are far below the Fermi level and thus only affect the Co $d_{xz,yz}$ states with minority spin. Effectively, Co-Cu hybridization drags down the Co $d_{xz,yz}$ states and enlarges the energy separations between the Co $d_{xz,yz}$ states and the unoccupied Co $d$ states. As a result,

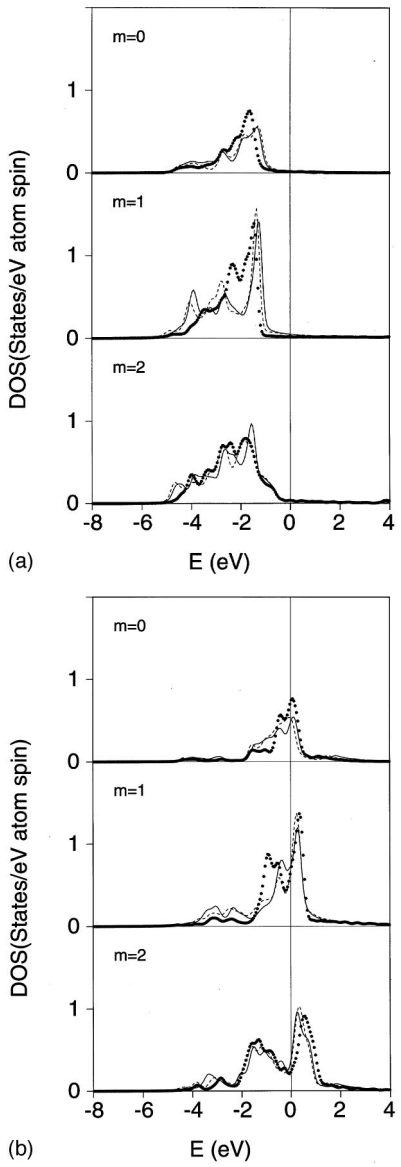


FIG. 8. The *m*-projected density of states for the Co *d* bands in Co/Cu(001) (dotted lines), Cu/Co/Cu(001) (solid lines), and 2Cu/Co/Cu(001) (dashed lines). The majority- and minority-spin parts are given in panels (a) and (b), respectively.

the negative contributions to $E_{MCA}$ are reduced. Meanwhile, the positive contributions to $E_{MCA}$ are mainly from the in-plane Co $d_{xy}$ and $d_{x^2-y^2}$ states, and thus are quite insensitive to the presence of Cu neighbors and finally prevail the negative contributions in Cu/Cu/Cu(001).

This mechanism is clearly shown in Fig. 8 by the *m*-projected density of states in the Co muffin-tin sphere. Since the Cu states are far below the Fermi level, they mainly hybridize with the occupied Co states. As expected, the DOS curve for the Co $d_{xz}$ and $d_{yz}$ states ($m=1$) is strongly affected by the surrounding Cu layers. The peak at $-1.2$ eV in Co/Cu(001) of the minority spin Co *d* band [cf. Fig. 8(b)] is split into three peaks at $-0.6$ eV, $-2.2$ eV, and $-3.0$ eV in the Cu/Co/Cu(001) and 2Cu/Co/Cu(001) systems, respectively. Meanwhile, the minority spin Co $d_{z^2}$ surface state in Co/Cu(001) gains some electrons and shift to the low-energy region. The SOC interaction between the minority-spin Co $d_{z^2}$ and Co $d_{xz,yz}$ states (through the $L_x$ operator) is reduced whereas that between the minority spin Co $d_{xz}$ and Co $d_{yz}$ states (through the $L_z$ operator) is enhanced. This thus results in a positive MCA energy. The second Cu overlayer, however, weakens this effect since the *m*-projected DOS curves of 2Cu/Co/Cu(001) are always between those of Co/Cu(001) and Cu/Co/Cu(001).

The calculated values of $K_2$ are positive for Co/Cu(001) (6 $\mu$eV) and Cu/Co/Cu(001) (11 $\mu$eV), which indicates that the easy axis is along the (110) direction in the cubic unit cell. In 2Cu/Co/Cu(001), $K_2$ changes to negative ($-1$ $\mu$eV). This means that the in-plane MCA energy is very sensitive to the environment even in the second neighbors. Experimentally, Krams *et al.*[2] found that the $K_2$ coefficient is almost independent of the Cu coverage. By contrast, more recent experiments by Weber and Hope *et al.*[5,6] observed significant changes in $K_2$ with the Cu coverage, even when it is as thick as 16 ML.

By comparing LDA and GGA results, we found that the gradient corrections affect the MCA energy strongly. Using the same atomic structures, LDA produces uniaxial MCA energies of $-0.36$ meV and $+0.69$ meV for Co/Cu(001) and Cu/Co/Cu(001), respectively. With the LDA-optimized structure, the value of $K_1$ for Co/Cu(001) is only $-0.12$ meV.[14]

From the LDA and GGA DOS curves for Cu/Co/Cu(001) in Fig. 5, the gradient corrections appear not to change the band structure much, especially for the Cu atoms. For Co, GGA slightly enhances the exchange splitting (by 0.1–0.2 eV) and weakens the Co/Cu interfacial interaction (cf. the reduction for the peaks at $-0.6$ eV, $-1.3$ eV, and $-3.2$ eV in the minority-spin DOS curves). By contrast, the calculated values of $K_1$ and $K_2$ for Cu/Co/Cu(001) in Fig. 7(b) appear to be very sensitive to the gradient corrections. Using the same atomic structure optimized through GGA calculations, LDA results of $K_1$ and $K_2$ curves deviate markedly from the GGA counterparts. Although the trends of $K_2$ curves appear to be very similar, LDA gives a very small in-plane anisotropy energy (1.2 $\mu$eV per Co atom). This is understandable since MCA energies mainly depend on the Co *d* states near the Fermi level. In our recent calculations, we also found significant discrepancies between LDA and GGA results of MCA energies in the free Ni and Fe monolayers.[8]

Clearly, the gradient corrections in GGA not only improve the results of structural optimizations for $3d$-transition metals, but alter their band structures also. Both effects have significant consequences for the determination of MCA energies. Comparing to the measured uniaxial $E_{MCA}$ available for Co/Cu(001), 0.38 meV per Co atom,[2] it appears that LDA produces a better agreement. However, one must view this agreement very cautiously since this value was extrapolated from data for samples with thicker Co layers. Further experimental measurements for $E_{MCA}$ of the Co/Cu(001) systems in the monolayer regime are desired.

## V. CONCLUSIONS

The FLAPW method with GGA is applied for the determination of structural, electronic, and magnetic properties of Co/Cu(001) systems with Cu cap layers. The GGA is found to improve the reliability of first-principles structure optimizations for $3d$ metals and to strongly alter results of MCA

energies. The calculated uniaxial MCA energies are $-0.61$ meV, $+0.54$ meV, and $+0.21$ meV for Co/Cu(001), Cu/Co/Cu(001), and 2Cu/Co/Cu(001), respectively. This explains the ''anomalous perpendicular anisotropy'' observed in Co/Cu and other systems.

## ACKNOWLEDGMENTS

This work was supported by the Office of Naval Research (Grant No. N0014-95-1-0489), and by computing grants at ARSC and NAVO through the ONR.

[1] P. A. Gacia, A. D. Meinholdt, and A. Suna, Appl. Phys. Lett. **47**, 178 (1985).
[2] P. Krams, F. Lauks, R. L. Stamps, B. Hillebrands, and G. Güntherodt, Phys. Rev. Lett. **69**, 3674 (1992).
[3] B. N. Engel, M. H. Wiedmann, and C. M. Falco, J. Appl. Phys. **75**, 6401 (1994).
[4] F. Huang, G. J. Mankey, and R. J. Willis, J. Appl. Phys. **75**, 6406 (1994).
[5] W. Weber, A. Bischof, R. Allenspach, C. H. Back, J. Fassbender, U. May, B. Schirmer, R. M. Jungblut, G. Güntherodt, and B. Hillebrandt, Phys. Rev. B **54**, 4075 (1996).
[6] S. Hope, E. Gu, B. Choi, and J. A. Bland, Phys. Rev. Lett. **80**, 1750 (1998).
[7] R. K. Kawakami, M. O. Bowen, H. J. Choi, E. J. Escorcis-Aparicio, and Z. Q. Qiu, Phys. Rev. B **58**, R5924 (1998).
[8] R. Q. Wu and A. J. Freeman, J. Magn. Magn. Mater. (to be published).
[9] D.-S. Wang, R. Q. Wu, and A. J. Freeman, Phys. Rev. Lett. **70**, 869 (1993).
[10] X. Wang, R. Wu, D.-S. Wang, and A. J. Freeman, Phys. Rev. B **54**, 61 (1996).
[11] L. Zhong, M. Kim, X. Wang, and A. J. Freeman, Phys. Rev. B **53**, 9770 (1996).
[12] M. Kim, L. Zhong, and A. J. Freeman, Phys. Rev. B **57**, 5271 (1998).
[13] L. Szunyogh, B. Ujfalussy, U. Pustogowa, and P. Weinberger, Phys. Rev. B **57**, 8838 (1998).
[14] R. Q. Wu and A. J. Freeman, J. Appl. Phys. **79**, 6500 (1996); R. Q. Wu, L. J. Chen, and A. J. Freeman, J. Magn. Magn. Mater. **170**, 103 (1997).
[15] A. B. Shick, D. L. Novikov, and A. J. Freeman, Phys. Rev. B **56**, R14 259 (1997).
[16] J. P. Perdew, K. Burke, and Y. Wang, Phys. Rev. B **54**, 16 533 (1996).
[17] E. Wimmer, H. Krakauer, M. Weinert, and A. J. Freeman, Phys. Rev. B **24**, 864 (1981), and references therein.
[18] J. A. C. Bland, G. A. Gehrig, B. Kaplan, and C. Daboo, J. Magn. Magn. Mater. **113**, 173 (1992).
[19] R. Q. Wu, L. J. Chen, A. B. Shick, and A. J. Freeman, J. Magn. Magn. Mater. **177**, 1216 (1998).
[20] T. Soma, Physica B & C **97**, 76 (1979).
[21] J. Stohr, R. Jaeger, and T. Kendelewicz, Phys. Rev. Lett. **49**, 142 (1982).
[22] M. Tischer, O. Hjortstam, D. Arvanitis, J. H. Dunn, F. May, K. Baberschke, J. Trygg, J. M. Wills, B. Johanson, and O. Eriksson, Phys. Rev. Lett. **75**, 1602 (1995).